

The abundance of satellites depends strongly on the morphology of the host galaxy

Pablo Ruiz ^{*}, Ignacio Trujillo^{1,2} and Esther Marmol-Queralto^{1,2,3}

¹Departamento de Astrofısica, Universidad de La Laguna, E-38205 La Laguna, Tenerife, Spain

²Instituto de Astrofısica de Canarias, c/ Vıa Lactea s/n, E-38205 La Laguna, Tenerife, Spain

³Institute for Astronomy, University of Edinburgh, Royal Observatory, Edinburgh EH9 3HJ, UK

Accepted 2015 September 1. Received 2015 August 21; in original form 2015 March 30

ABSTRACT

Using the spectroscopic catalogue of the Sloan Digital Sky Survey Data Release 10, we have explored the abundance of satellites around a sample of 254 massive ($10^{11} < M_{\star} < 2 \times 10^{11} M_{\odot}$) local ($z < 0.025$) galaxies. We have divided our sample into four morphological groups (E, S0, Sa, Sb/c). We find that the number of satellites with $M_{\star} \geq 10^9 M_{\odot}$ and $R < 300$ kpc depends drastically on the morphology of the central galaxy. The average number of satellites per galaxy host ($N_{\text{Sat}}/N_{\text{Host}}$) down to a mass ratio of 1:100 is: 4.5 ± 0.3 for E hosts, 2.6 ± 0.2 for S0, 1.5 ± 0.1 for Sa and 1.2 ± 0.2 for Sb/c. The amount of stellar mass enclosed by the satellites around massive E-type galaxies is a factor of 2, 4 and 5 larger than the mass in the satellites of S0, Sa and Sb/c-types, respectively. If these satellites would eventually infall into the host galaxies, for all the morphological types, the merger channel will be largely dominated by satellites with a mass ratio satellite-host $\mu > 0.1$. The fact that massive elliptical galaxies have a significant larger number of satellites than massive spirals could point out that elliptical galaxies inhabit heavier dark matter haloes than equally massive galaxies with later morphological types. If this hypothesis is correct, the dark matter haloes of late-type spiral galaxies are a factor of ~ 2 –3 more efficient on producing galaxies with the same stellar mass than those dark matter haloes of early-type galaxies.

Key words: galaxies: abundances – galaxies: elliptical and lenticular, cD – galaxies: evolution – galaxies: formation – galaxies: luminosity function, mass function – galaxies: spiral

1 INTRODUCTION

Galaxy mergers have been raised in the last years as the most likely channel of size and mass growth of massive ($M_{\star} \geq 10^{11} M_{\odot}$) galaxies through cosmic time. Numerous observational and theoretical studies support this mode of growth, a mechanism that has increased the size and mass of the massive galaxies during the last ~ 11 Gyr. In this scenario, the ancestors of the present-day most massive galaxies created the bulk of their mass in a short but very intense starburst event at $z \gtrsim 2$ (e.g. Kereš et al. 2005; Dekel et al. 2009; Oser et al. 2010; Ricciardelli et al. 2010; Wuyts et al. 2010; Bournaud et al. 2011) having, in that first evolutionary stage, a structure more compact. Later, a progressive process of mergers with satellites produced the envelopes that we see today surrounding these galaxies (Kochfar & Silk 2006; Oser et al. 2010; Feldmann et al. 2011). Many works support the above scheme, finding evidences for a continuous size evolution of the massive galaxies since $z \sim 3$ (e.g. Trujillo et al. 2007; Buitrago et al. 2008) mainly produced by the formation of the outer most regions (e.g.

Bezanson et al. 2009; Hopkins et al. 2009a; Carrasco et al. 2010; van Dokkum et al. 2010; Montes et al. 2014). In addition, other authors have found that the average velocity dispersion of the massive galaxies have decreased mildly since $z \sim 2$ as expected theoretically from the galaxy merger scenario (e.g. Cenarro & Trujillo 2009). Other observations point out that this size evolution of the massive galaxies does not depend on the age of the stellar population (Trujillo et al. 2011) nor on their intrinsic sizes (Dıaz-Garcıa et al. 2013). This suggests a growth engine external to the galaxy properties. The absence of a significant number of relic galaxies in the nearby Universe also favours a merging scenario (e.g. Trujillo et al. 2009, 2014; Taylor et al. 2010).

The above merging scenario can be alternatively probed measuring the satellite abundances around massive galaxies as cosmic time flows (e.g. Newman et al. 2012). There are many works that have studied in detail the properties of the satellite galaxies over time (Jackson et al. 2010; Nierenberg et al. 2011, 2013; Man et al. 2012; Marmol-Queralto et al. 2012, 2013; Newman et al. 2012; Huertas-Company et al. 2013; Ferreras et al. 2014). In particular, Marmol-Queralto et al. (2012) found that the fraction of massive galaxies with satellites of a given mass ratio (1:100 up to $z =$

* E-mail: ruihern@gmail.com

1 and 1:10 up to $z = 2$) have remained constant with time. A behaviour which is in qualitative good agreement with semi-analytical predictions based on the Λ cold dark matter (Λ CDM) model (Quilis & Trujillo 2012). However, the semi-analytical models over-predict the fraction of massive galaxies with satellites down to 1:100 mass ratio by a factor of ~ 2 .

Parameters such as the abundance of satellites, their distribution or their intrinsic properties are intimately bound up with their host merger histories. These properties are thus, closely related to the underlying cosmology and they can be used to establish useful constraints to the models. The colours and structural properties of the host galaxies can be modified by gravitational interactions with their satellites. The main goal of this work is to analyse the relation between the abundance of satellites and the host morphology in a sample of nearby massive ($\sim 10^{11} M_{\odot}$) galaxies. We segregate our sample of galaxies in four groups which are representative of different structural configurations. Our morphological classification identifies visually the groups E, S0, Sa and Sb/c to explore the correlation between the number of satellites and the morphology of the host. Our approach differs from previous studies based on colours (Chen 2008; Guo et al. 2011b; Wang & White 2012), or those based on more general grouping (e.g. early-, late- or spheroid- disc like) of the massive galaxies (e.g. Guo et al. 2011b; Marmol-Queralto et al. 2012; Nierenberg et al. 2012).

Our samples of massive galaxies could be used in future works to test the Λ CDM predictions about the number of satellites surrounding the most massive galaxies in the present-day Universe (see e.g. Chen 2008; Liu et al. 2011; Wang & White 2012) according to their morphology. Our study also allows us to explore which is the most likely merging channel of present-day massive galaxies, i.e. which type of satellites contribute most to the mass increase of their host galaxies in case they eventually merge with its main object. Consequently, this local study, along with other works at higher z (see e.g. Ferreras et al. 2014), allows us to explore whether the merging channel has changed with time and its dependence with the host morphology.

This paper is structured as follows. In Section 2, we describe our sample of hosts and satellite galaxies, their completeness and their stellar mass estimates. Section 3 explains the satellite selection criteria and the methods used to clean our sample from background and clustering contamination. Our results concerning the satellite abundances of the distinct samples are presented in Section 4. Section 5 discusses the main results of this paper and finally our work is summarized in Section 6. Hereafter, we assume a cosmology with $\Omega_m = 0.3$, $\Omega_{\Lambda} = 0.7$ and $H_0 = 70 \text{ km s}^{-1} \text{ Mpc}^{-1}$.

2 THE DATA

In this paper, we use the ‘specphoto’ spectroscopic catalogue of Sloan Digital Sky Survey (SDSS) Data Release 10 (DR10; Ahn et al. 2014) to explore the abundance of satellites around a sample of massive galaxies in the nearby Universe ($z \leq 0.025$). The spectroscopic completeness of this catalogue is 90 per cent down to $r = 17.7$ mag. The catalogue includes a total of 1507954 Baryonic Oscillation Spectroscopic Survey (BOSS) spectra comprising 927844 galaxy spectra, 182009 quasar spectra and 159327 stellar spectra selected over 6373.2 deg^2 . We select those objects labelled as ‘GALAXY’ within the data set ‘specphoto’. This subset only has galaxies where the ‘SpecObj’ is a ‘sciencePrimary’ object, and the BEST PhotoObj is a PRIMARY.

We structure this section as follows. First, we show the proce-

dures to estimate the stellar masses of the galaxies of the catalogue. Then, we describe the selection of our host galaxies, the catalogue of potential satellites and finally, we study the completeness of our satellite population.

2.1 The stellar mass estimation

One of the goals of this work is to analyse the abundance of satellites as a function of the mass ratio satellite–host. To estimate the stellar masses, we use the Bell et al. (2003)’s recipe, assuming a Kroupa (2001) initial mass function (IMF). We take the ‘model-Mag’ g - and r -band magnitudes from the ‘specphoto’ SDSS DR10 catalogue once they have been corrected from Galactic extinction (Schlegel et al. 1998). Then, we estimate the mass-to-light (M/L) ratio from the rest-frame $g-r$ colour, being the M/L ratio estimated in the r band as follows:

$$\log(M/L)_r = a_r + b_r(g-r) - 0.15, \quad (1)$$

where $a_r = -0.306$ and $b_r = 1.097$ are the coefficients applied for determining the M/L ratio in the r band and 0.15 is subtracted to match the results to a Kroupa IMF.

Using these computed $(M/L)_r$, we can directly estimate the stellar masses using the next relationship:

$$\log(M/M_{\odot}) = \log(M/L)_r - 0.4(M_r - M_{\odot,r}), \quad (2)$$

where M_r is the absolute magnitude of the galaxy and $M_{\odot,r} = 4.68$ the absolute magnitude of the Sun in the SDSS r band. Given that our study is focused on objects at very low redshift, we do not apply K -corrections to the above g and r magnitudes since it will not affect significantly our mass estimates. In fact, the expected values for K -corrections at $z < 0.025$ are typically below ~ 1 per cent relative to calibration errors found for g and r filters in the photometry of SDSS DR10 (Padmanabhan et al. 2008).

To test how reliable our stellar mass estimates based on colours are, we have compared our stellar masses with those from Nair & Abraham (2010) based on Kauffmann et al. (2003). This comparison can be done only for a subset of the galaxies in our catalogue. As the result of this comparison we find a bias of 0.2 dex Nair & Abraham (being the 2010, smaller) with a typical uncertainty of 0.1 dex among the two stellar mass estimators. On what follows, we take that uncertainty as representative of our error estimation of the stellar mass. The above bias is not surprising taking into account the different methodologies and stellar population models used in both estimates of the stellar mass.

2.2 The sample of host galaxies

Using the available data, we estimate the stellar mass of our galaxies as we explained above (Section 2.1). To build our sample of massive host galaxies, we select only the galaxies with $M_{\star} \geq 10^{11} M_{\odot}$. We limit our sample to galaxies with $z < 0.025$ (i.e. at a distance ≤ 100 Mpc). The average apparent r band magnitude of our host galaxies is $r \sim 13$ mag. This implies, taking into account the spectroscopic completeness limit of our catalogue, that we can identify potential satellites with stellar masses 100 times less massive than their hosts. We have discarded massive hosts whose M/L (as computed by their $g-r$ colour) were unreasonable (i.e. out of the interval $0.1 < (M/L)_r < 4$) and those ones with large photometric errors. The percentage of massive galaxies discarded by these reasons were 5 per cent. We also check visually our sample of massive galaxies to reject objects wrongly labelled as galaxies

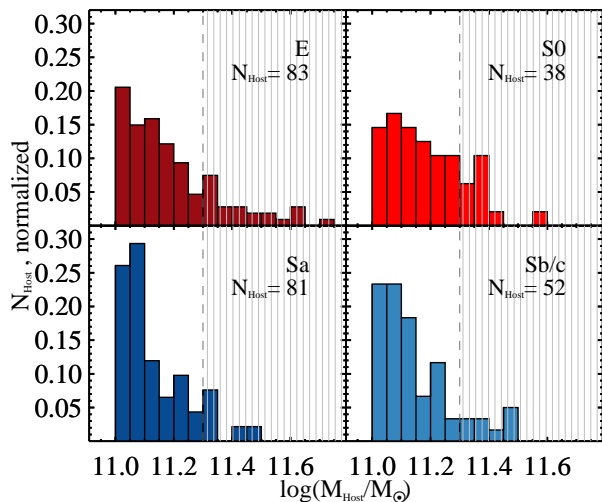


Figure 1. Distribution of the normalized stellar mass for the host of each morphological type. The upper left-hand panel corresponds to the massive E type, the upper right to S0 type, the lower left to Sa and the lower right to the Sb/c massive galaxies. The non-stripped area illustrates the distribution of massive galaxies chosen ($10^{11} < M_{\star}/M_{\odot} < 2 \times 10^{11}$) for this work. The N_{Host} label in the panels indicates the number of host found within that stellar mass interval.

as well as those ones in clear interaction with another galaxy. Also, to avoid incompleteness in the number of satellites due to area coverage, 27 massive galaxies were additionally discarded due to their proximity to the edge of the SDSS DR10 spectroscopic footprint.

Finally, the mass distribution of the different morphological types was checked. Our morphological segregation is explained in the next subsection. The distribution of the mass of the hosts is illustrated in the Fig. 1 and shows a high-mass-tail for the massive ellipticals which is not so prominent for the rest of galaxy types. To avoid any potential bias caused by this different mass distribution of the hosts, we established an upper mass limit of $2 \times 10^{11} M_{\odot}$. Thus, our final host sample is composed of 254 massive galaxies.

The main goal of this work is to study the local abundance of satellites as a function of the morphological type of the massive hosts. Unlike other studies whose separation is based on colours, we do our own visual classification based on the Hubble classification using the SDSS DR10 images (see next subsection). Within the mass range ($10^{11} < M_{\star}/M_{\odot} < 2 \times 10^{11}$) we find 83 E-type, 38 S0-type, 81 Sa-type and 52 Sb/c-type galaxies. Fig. 2 illustrates some of our host galaxies. Our visual classification is compared with the one done by Nair & Abraham (2010) for 89 massive galaxies we have in common. We find an agreement of 84 per cent.

2.2.1 Sorting the galaxy hosts into morphological classes

In this work we have segregated our galaxies into four different morphological types (E, S0, Sa and Sb/c). The physical motivation for sorting into these four categories is related to the expected strong connection between the evolutionary path followed by the galaxies and their detailed morphologies. This connection leaves their imprints on the relation between the specific angular momentum of the galaxies, at a fixed stellar mass, and the galaxy morphology (see e.g. Romanowsky & Fall 2012). This link can also be seen in the different shape of the outermost regions of the galaxies de-

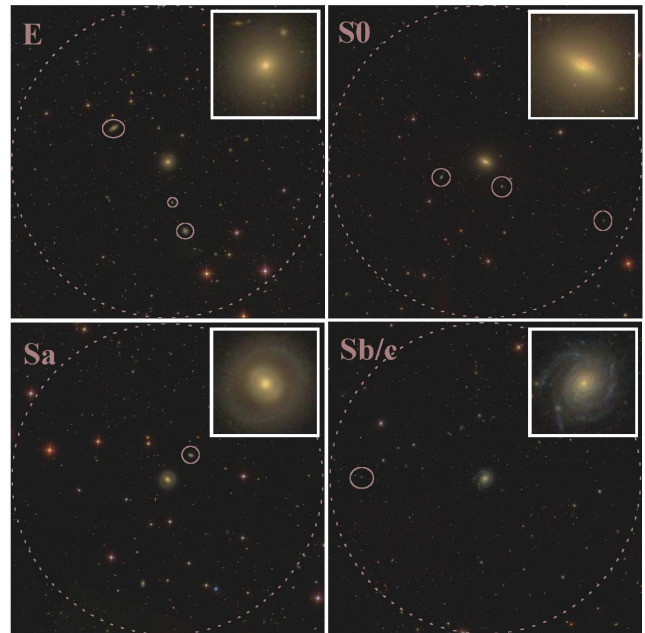


Figure 2. Four examples of massive galaxies in our sample and their surroundings. The dashed circles enclose a region of 300 kpc in radius. The small circles indicate the position of the satellites. The upper right-hand panels are a zoom-in of the host galaxies to illustrate their morphologies.

pending on the global morphological type (e.g. Pohlen & Trujillo 2006; Erwin et al. 2008). If as expected, the merging activity of the galaxies is connected to the galaxy morphology, a natural prediction is that the number of satellites surrounding the galaxies should be also related with the shape of their host galaxies. It is worth noting that the merging activity is likely linked to the amount of mass contained within the bulge of the galaxies (e.g. Hernquist & Barnes 1991; Steinmetz & Muller 1995; Fu et al. 2003; Zavala et al. 2008; Kroupa et al. 2010; Kroupa 2012). The prominence of the bulge is one of the key ingredients in the galaxy morphological criteria, and consequently, a detailed segregation among the morphological types (beyond a disc/elliptical separation) could be connected with the number of satellites around the host galaxies.

To classify our galaxies we have followed the traditional Hubble classification scheme. For all our galaxies, we look in detail the colour stamps provided for each of them by the finding chart tool of SDSS. To disentangle among ellipticals and S0s, we search for any evidence of a less steeply declining brightness in the outer region of the galaxies beyond the central brightness condensation. In cases where the inclination of the disc component of the S0 galaxy was clearly showing a flat outer structure or when some dust features were obvious, the distinction between the two galaxy types was relatively simple. Among the disc galaxy population, the segregation between Sa and Sb/c was done according to the relevance of the bulge in producing the overall light distribution as well as exploring the properties of the spiral arm structure, i.e. the tightness with which the spiral arms are wound and the number of substructure visible in those features.

2.3 The sample of satellite galaxies

To select our sample of potential satellites, we also use the ‘specphoto’ catalogue of SDSS DR10. Our satellites are those galaxies in the catalogue which fulfil the proximity criteria (i.e.

projected distance to the hosts) and stellar mass criteria that we will explain in the next section (Section 3).

On building our sample of satellites, we have to prevent the inclusion of objects with deficient measurement of its colour because this would lead to a wrong estimate of its stellar mass. To conduct this task, we need to account for the photometric errors both in g and r bands to assure the colour is measured with enough confidence. For this reason, in addition to the magnitude limit in the r band we have used above, we also demand that the photometric error at estimating the number counts of each galaxy will be less than 5σ the expected error at measuring their number counts. In other words, acceptable photometric error for each object for us are those whose $\text{error}(\text{counts})$ is $\leq 5 \times \sqrt{\text{counts} + \sigma_{\text{sky}}^2}$, with σ_{sky} the uncertainty (in counts) at measuring the sky value in each band. We find as typical values for the sky in the SDSS images 24.88 counts (g band) and 23.96 counts (r band). We have used the following set of equations to transform our magnitudes and $\text{error}(\text{mag})$ provided by the catalogues into counts and $\text{error}(\text{counts})$:

$$\text{mag} = -2.5 \log \left(\frac{\text{counts}}{\text{exptime}} 10^{0.4(aa+kk \times \text{airmass})} \right) \quad (3)$$

$$\text{error}(\text{mag}) = \frac{2.5}{\ln 10} \frac{\text{error}(\text{counts})}{\text{counts}} \quad (4)$$

with $\text{exptime}=53.907$ s and aa , kk and airmass provided for each object, being aa and kk the values of the zero-point and the extinction coefficient respectively. Those galaxies in our catalogue which show a photometric error larger than those values (in any of the two bands) are discarded from the analysis since these ones could be linked to artefacts in the image, proximity to bright nearby companions, etc. We have estimated the number of galaxies rejected because of large photometric errors, finding that less than 0.5 per cent of the objects are discarded, a reasonable result since these objects are relatively bright.

2.3.1 The completeness of the satellite sample

Once the stellar masses of the galaxies of our catalogue are determined, we can estimate down to which stellar mass the catalogue is complete. The stellar mass limit for completeness is a function of the redshift (see Fig. 3). To explore the degree of completeness of satellites down to $M_{\star} \sim 10^9 M_{\odot}$, we have used our most distant redshift interval $0.023 < z < 0.025$. The peak on the mass distribution of the galaxies in the catalogue at $z \sim 0.024$ is $\log(M_{\star}/M_{\odot}) \sim 8.95$. If we now take into account that the minimum stellar mass that we have fixed for our hosts ($\log(M_{\star}/M_{\odot}) \sim 11.0$), we should be able to study with completeness satellites whose $M_{\text{Sat}}/M_{\text{Host}} \geq 0.01$.

However, it is worth noting that there is a potential bias to miss the oldest satellites at a fixed stellar mass. This is because the catalogue is complete in redshift down to a given apparent r -band magnitude ($r \sim 17.7$). That value translates into the following absolute magnitude for the sample at $z=0.025$: $M_r = -17.65$ mag. To transform this absolute magnitude into a stellar mass limit we need to have an estimation of the stellar M/L ratio of our satellites. To do this, we assume a conservative age for the less massive galaxies of 10 Gyr. Using the MIUSCAT spectral energy distributions SEDs developed by Vazdekis et al. (2012) and Ricciardelli et al. (2012), a solar metallicity and a Kroupa IMF, the $(M/L)_r$ ratio for these objects is around 3. This translates into the following stellar mass: $\log(M_{\star}/M_{\odot}) \sim 9.41$ (i.e. a mass ratio satellite–host of 1:40).

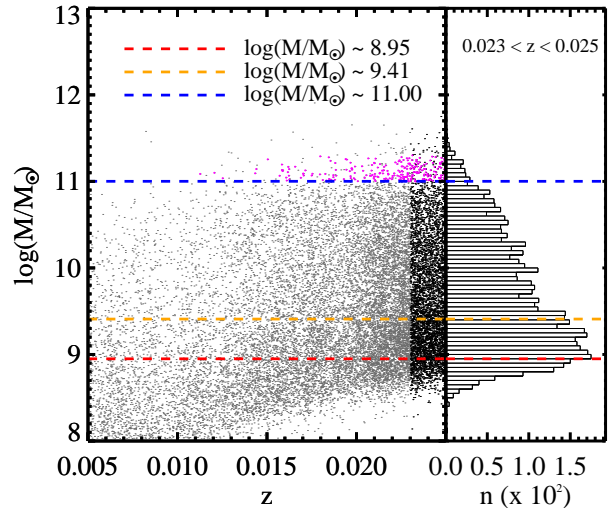


Figure 3. Left-hand panel: the points in grey correspond to stellar mass distribution versus redshift for all the galaxies in the ‘specphoto’ SDSS DR10 catalogue. The pink points represent our sample of massive host galaxies. The black points indicate those objects in the right-hand panel within the redshift ($0.023 < z < 0.025$) used to estimate the stellar mass completeness. Right-hand panel: stellar mass distribution for the spectroscopic catalogue in the redshift interval $0.023 < z < 0.025$. The red dashed line is the completeness limit $\sim 8.9 \times 10^8 M_{\odot}$ whereas the blue line represents the minimum stellar mass for the sample of massive galaxies ($10^{11} M_{\odot}$). A conservative estimation for the stellar mass completeness of the spectroscopic sample is showed by the orange dashed line: $\sim 2.6 \times 10^9 M_{\odot}$ (see text for details).

On what follows, we will consider this value as the most conservative mass completeness limit of our satellite galaxies.

3 SATELLITE SELECTION CRITERIA

Our criteria to search for potential satellites around the host sample are based on the next three steps.

(i) We detect all the galaxies in the ‘specphoto’ SDSS DR10 catalogue which are within a projected radial distance to our central galaxies of $R = 300$ kpc. We only consider those host galaxies when the area enclosed by the search radius of satellites is fully contained within the catalogue borders. As we mentioned above, 27 hosts were discarded due to their proximity to the catalogue edge. Our adopted search radius of 300 kpc is a compromise between having a large area for finding a significant number of satellite candidates gravitationally bound to our central massive galaxies but not as large as to be severely contaminated by background and foreground objects (see Section 3.1).

(ii) The absolute difference between satellite redshifts and the redshift of the central galaxies must be lower than 1000 km s^{-1} . This value has been used before in the literature to select gravitationally bound satellites of massive galaxies (see e.g. Wang & White 2012; Ruiz, Trujillo & Marmol-Queralto 2014). The velocity distribution of the galaxies around the massive host galaxies selected that way is close to a Gaussian shape with a dispersion of 300 km s^{-1} . Consequently, our criteria enclose the vast majority of satellites around the massive galaxies.

(iii) The mass ratio between our host massive galaxy and the satellite should be above 1:100.

Those objects which fulfil the above criteria are counted as

potential satellites of their hosts. The number of satellites observed around a host sample is defined as N_{Obs} . Before showing our results, we will address the potential biases that can affect our counting of satellites around the massive hosts.

3.1 Background correction

Despite we have used spectroscopic redshift information to select our potential satellite galaxies, there is still a fraction of objects that satisfy all the above criteria but are not gravitationally bound to our massive galaxies. These objects are counted as satellites because the uncertainties on their redshift estimates include them within our searching redshift range. These foreground and background objects (hereafter we will use the term background to refer to both of them) constitute an important source of uncertainty in this kind of studies. Consequently, it is key to estimate accurately the background contamination in order to statistically subtract its contribution from the number of galaxies hosting satellites.

To estimate the typical number of background objects that contaminates our satellite samples, we have developed a set of simulations. The procedure consists on placing a number of mock galaxies (equal to the number of our host galaxies) randomly through the volume of the catalogue conserving their original values in the stellar mass and redshift of the sample of massive galaxies. Once we have placed our mock galaxies through the catalogue, we count which number of these galaxies have fake satellites around them taking into account the criteria of stellar mass, redshift and distance explained in the above section. This procedure is repeated 2000 times to have a robust estimate of the number of 'satellites' around the mock host galaxies. We define this average number as N_S . Then, being N_{Obs} the number of observed satellite galaxies around either of our host massive galaxies, we correct statistically its excess subtracting the number of satellites representative of the background (N_S), such as it is shown in the equation below (equation 5). By construction, N_S is independent on the morphology of the host.

$$N_{\text{Sat,S}} = N_{\text{Obs}} - N_S \quad (5)$$

To take into account that the environmental density and the morphology are linked for massive nearby galaxies, we also compute a clustering correction as explained in the following section.

3.2 Clustering correction

At low redshift, the over density regions are specially populated by massive galaxies. It is worth therefore exploring whether our background correction is representative of the contamination of sources surrounding our host galaxies or whether it is necessary to compute the excess of probability of finding 'satellites' in these environments. We term this as clustering.

Being the clustering an effect associated with the region surrounding the hosts, ideally one would like to measure its influence as closer as possible to the host. In practice, this is done by measuring the amount of satellite candidates in different annuli beyond our search radius (Chen et al. 2006; Liu et al. 2011; Marmol-Queralto et al. 2012; Ruiz, Trujillo & Marmol-Queralto 2014). We denote N_C as the number of 'satellite' galaxies placed in these annuli which fulfil our selection criteria for each morphological host type. N_C is a measurement of the background contamination plus the excess over this background caused by the clustering. This method has the disadvantage, compared to the simulations that

we have conducted above, that is statistically more uncertain since N_C can be measured only around our massive galaxies and their number is relatively small.

To quantify the effect of the clustering, we count the number N_C of satellites observed in annuli between 500 and 600 kpc which fulfil our selection criteria. The size of each annuli has the same area that our main exploration area around the hosts [i.e. $\pi (300 \text{ kpc})^2$]. As it was done in the above section, we subtract N_C to the number of observed satellites N_{Obs} to correct for the statistic excess given by the clustering in the sample of observed satellites. In other words:

$$N_{\text{Sat,C}} = N_{\text{Obs}} - N_C \quad (6)$$

The radial range 500-600 kpc for determining the clustering is a compromise among having a local measurement of the environment around our massive host galaxies but being far away enough such as the probability of finding a gravitationally bounded satellite to our targeted galaxy will be low. The projected radial distance of 500 kpc is chosen following many works in the literature (e.g. Sales & Lambas 2004, 2005; Chen et al. 2006; Bailin et al. 2008; Wang & White 2012; Ruiz, Trujillo & Marmol-Queralto 2014) which have used only galaxies with radial distances lower than 500 kpc to define their sample of truly (i.e. bounded) satellite galaxies.

4 RESULTS

4.1 Cumulative number of satellites per galaxy host

The abundance of satellites is quantified using the number of satellites per number of massive galaxies $N_{\text{Sat}}/N_{\text{Host}}$ down to a mass ratio satellite-host of 1:100. The results are shown in the left-hand panel of the Fig. 4 and Table 1. In addition to explore our satellites in a search radius of 300 kpc, we repeat the same exercise using a 100 kpc radius to compare with previous results in the literature.

The $N_{\text{Sat}}/N_{\text{Host}}$ values have been corrected from contaminants by subtracting to N_{Obs} the quantities N_S and N_C found in the background simulation and in our estimates of clustering, respectively. The uncertainties of N_{Obs} and N_C were estimated from bootstrap resamplings of host sample sets. As we can see in Table 1, the background contamination is very low since our work uses spectroscopic redshifts. According to that table, the maximum contamination expected by the background is ~ 0.1 satellites per galaxy host. The ratios N_S/N_{Host} and N_C/N_{Host} in Table 1 show that the background contamination is, as expected, quite independent on the morphological type. However, if we compare the typical number of fake satellites due to clustering (N_C/N_{Host}), we see significant differences. By far, the host galaxies that are more likely affected by contaminants are the E-type. On one hand, we have to take into account that the massive Sb/c-types are not usually expected to be into the cluster's core regions. Thus, if we compare both N_S/N_{Host} and N_C/N_{Host} around the massive Sb/c-types, we find a factor of 6 larger contamination due to clustering than due to background. In contrast, this ratio increases dramatically up to ~ 16 times for the elliptical hosts. S0 and Sa-types show a ratio of ~ 7 -8 and ~ 6 -7, respectively, a factor similar to the one found around Sb/c-types. It is remarkable that the density of objects at assessing the clustering and the background contaminant around the Sb/c-types, although close, are not similar. All this indicates that these massive galaxies are immersed in an environment similar to the samples of S0 and Sa and therefore, they are not completely isolated.

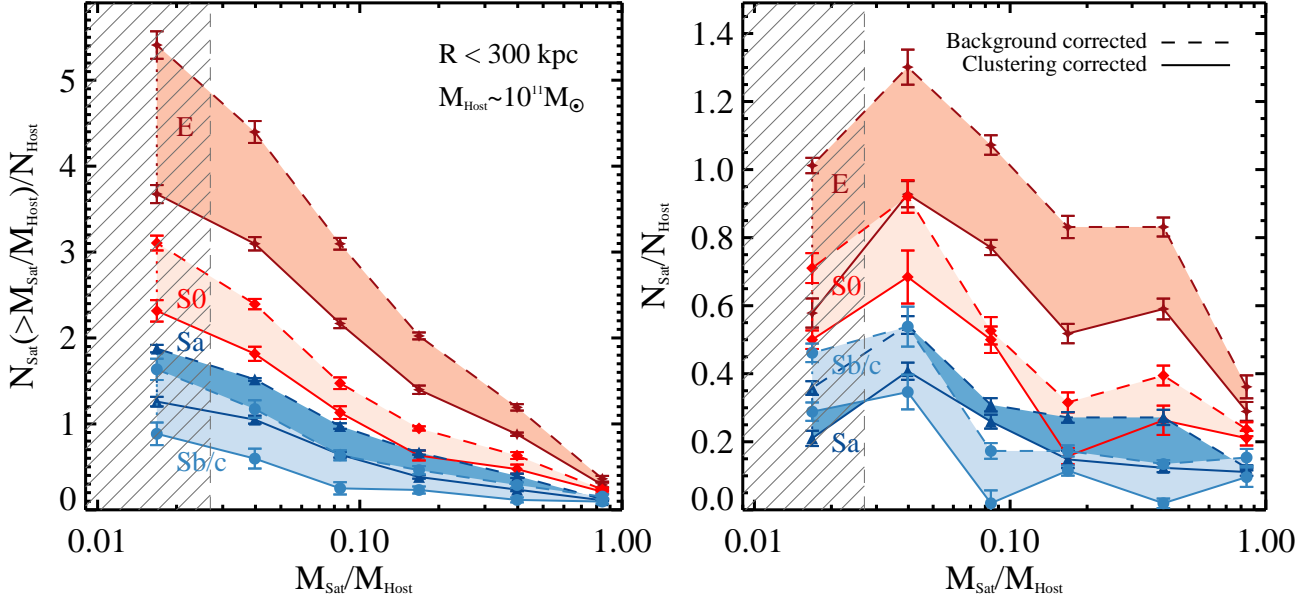


Figure 4. Left-hand panel: cumulative number of satellites per galaxy host for each morphological type versus the stellar mass ratio satellite-host down to 1:100. The dark red lines correspond to centrals E type, red to S0 type, dark blue to Sa type and soft blue to Sb/c type. The coloured areas represent the space between the abundance estimated after applying background and clustering corrections. The dashed lines correspond to the background correction and the continuous line to the clustering. The striped grey region indicates our more conservative measure of the completeness ($\sim 1:40$) – see Section 2.3.1. Right-hand panel: differential number of satellites per galaxy host for each of the morphological type versus the stellar mass ratio satellite–host. The colour code associated with the lines is the same that in the left-hand panel.

Focusing on the satellite abundances, we find that the number of satellites per galaxy host is 1.4-2.0 when we explore satellites down to a mass ratio 1:10 around massive elliptical galaxies. If we increase that range of mass ratio down to 1:100, we find 3.7-5.4. The other morphological types show less number of satellites than in the E-host case. The more extreme case is found at comparing with the massive Sb/c type, their number of satellites per galaxy host grows between 0.23-0.46 and 0.88-1.63 from 1:10 to 1:100. Consequently, the massive E hosts have ~ 5 times more satellites than the massive Sb/c down to 1:10. A difference which declines up to 3-4 times in the case 1:100. At comparing $N_{\text{Sat}}/N_{\text{Host}}$ down to 1:10 with the other samples of galaxies, we find that the S0 and Sa types host ~ 2 and 3 times less satellites, respectively than the E types. At extending our search down to 1:100, that difference among the S0–Sa types and ellipticals barely change. When we restrict our satellite search up to only 100 kpc, the difference in the number of satellites among the different morphological types remains similar. As expected, the total number of satellites decreases when comparing a search radius of 300 kpc to one of 100 kpc. The decreasing factor is 2.5, 2.9, 2.2 and 3.5 for the E, S0, Sa and Sb/c types, respectively.

4.2 Differential number of satellites per galaxy host

We have also explored different intervals of the mass ratio satellite–host. The intervals are defined as 1:1-1:2, 1:2-1:5, 1:5-1:10, 1:10-1:20, 1:20-1:50, 1:50-1:100 and the number of satellites per host is illustrated in the right-hand panel of the Fig. 4 and Table 2. This ‘differential’ test allows us to compare how is distributed the population of satellites respect to their stellar mass.

As the results presented above, the dependence of the abundance of satellites with the morphology of the host is also appre-

ciable. In general, the massive ellipticals have more satellites, followed by S0, Sa and Sb/c types.

As shown in Table 2, the number of fake satellites per host due to the background $N_{\text{S}}/N_{\text{Host}}$ remains independently on the morphological type whereas the contamination due to the clustering $N_{\text{C}}/N_{\text{Host}}$ is prominently larger in the elliptical case and very similar among the types S0, Sa and Sb/c.

4.3 The amount of mass surrounding the galaxy hosts

We have studied the amount of stellar mass accumulated by the satellites around our samples of massive galaxies. This is estimated down to 1:100 and as a function of their projected distances to the central galaxy. This cumulative stellar mass of the satellites is measured summing the stellar mass of all the satellites down to 1:100 in each interval of the search radius up to 300 kpc and then, subtracting the amount of stellar mass in the fake satellites from the background simulations. To apply the clustering correction on the amount of stellar mass enclosed by the satellites, we estimate the amount of mass in ‘satellites’ in the interval 500-600 kpc using an annuli with the same projected area than the ones used to study this quantity (i.e. from $\pi 50^2$ to $\pi 300^2$). The results are illustrated in Fig. 5.

E-type massive galaxies are surrounded by a factor of 2-5 more stellar mass respect to the rest of morphological types. If we repeat this exercise using only satellites up to 100 kpc, the stellar mass accumulated for lenticulars and spirals is similar, however, it is still a factor of 2-6 lower than the mass collected by ellipticals. Among the early types, the ratio of mass surrounding ellipticals to the mass surrounding lenticulars is typically placed around a factor of 2 larger. The spiral types show a more gradual accumulation of stellar mass with radius. It is worth noting that the amount of stellar mass enclosed by the satellites of massive ellipticals is almost

Table 1. Cumulative number of satellites per host galaxy using the background ($N_{\text{Sat,S}}/N_{\text{Host}}$) and clustering corrections ($N_{\text{Sat,C}}/N_{\text{Host}}$) within a radial distance of 300 kpc and down to a mass ratio satellite-host 1:100. $N_{\text{Obs}}/N_{\text{Host}}$ is the observed number of satellites per host. $N_{\text{S}}/N_{\text{Host}}$ is the number of satellites per host in our background simulation and $N_{\text{C}}/N_{\text{Host}}$ the number of satellites per host within 500-600 kpc in our clustering analysis. The background and clustering corrections are estimated for each morphological type as it is shown in the table.

$M_{\text{Sat}}/M_{\text{Host}}$	$N_{\text{Obs}}/N_{\text{Host}}$	$N_{\text{S}}/N_{\text{Host}}$	$N_{\text{C}}/N_{\text{Host}}$	$N_{\text{Sat,S}}/N_{\text{Host}}$	$N_{\text{Sat,C}}/N_{\text{Host}}$
E					
0.50-1.0	0.40 ± 0.03	0.006 ± 0.0001	0.080 ± 0.008	0.36 ± 0.03	0.29 ± 0.03
0.20-1.0	1.23 ± 0.04	0.021 ± 0.0002	0.325 ± 0.022	1.19 ± 0.04	0.88 ± 0.02
0.10-1.0	1.94 ± 0.04	0.038 ± 0.0003	0.647 ± 0.046	2.02 ± 0.04	1.40 ± 0.05
0.05-1.0	3.14 ± 0.08	0.056 ± 0.0004	0.985 ± 0.061	3.10 ± 0.07	2.17 ± 0.05
0.02-1.0	4.44 ± 0.11	0.085 ± 0.0008	1.373 ± 0.083	4.40 ± 0.13	3.10 ± 0.08
0.01-1.0	5.51 ± 0.16	0.113 ± 0.0010	1.840 ± 0.105	5.41 ± 0.16	3.67 ± 0.11
S0					
0.50-1.0	0.23 ± 0.02	0.005 ± 0.0001	0.032 ± 0.010	0.24 ± 0.02	0.21 ± 0.02
0.20-1.0	0.64 ± 0.04	0.020 ± 0.0003	0.168 ± 0.019	0.63 ± 0.04	0.47 ± 0.05
0.10-1.0	0.90 ± 0.02	0.037 ± 0.0006	0.329 ± 0.019	0.95 ± 0.02	0.63 ± 0.06
0.05-1.0	1.40 ± 0.07	0.056 ± 0.0008	0.346 ± 0.020	1.47 ± 0.07	1.13 ± 0.07
0.02-1.0	2.35 ± 0.06	0.084 ± 0.0012	0.629 ± 0.040	2.39 ± 0.06	1.82 ± 0.08
0.01-1.0	2.99 ± 0.09	0.113 ± 0.0016	0.804 ± 0.043	3.11 ± 0.09	2.32 ± 0.12
Sa					
0.50-1.0	0.11 ± 0.01	0.006 ± 0.0001	0.017 ± 0.003	0.12 ± 0.01	0.11 ± 0.01
0.20-1.0	0.41 ± 0.03	0.022 ± 0.0002	0.164 ± 0.014	0.40 ± 0.03	0.23 ± 0.02
0.10-1.0	0.67 ± 0.03	0.039 ± 0.0003	0.301 ± 0.033	0.67 ± 0.03	0.38 ± 0.02
0.05-1.0	0.97 ± 0.03	0.057 ± 0.0004	0.349 ± 0.037	0.98 ± 0.03	0.64 ± 0.03
0.02-1.0	1.45 ± 0.02	0.086 ± 0.0006	0.492 ± 0.053	1.52 ± 0.02	1.05 ± 0.05
0.01-1.0	1.89 ± 0.04	0.115 ± 0.0008	0.662 ± 0.056	1.88 ± 0.04	1.26 ± 0.06
Sb/c					
0.50-1.0	0.13 ± 0.03	0.006 ± 0.0001	0.041 ± 0.008	0.15 ± 0.03	0.10 ± 0.03
0.20-1.0	0.26 ± 0.03	0.022 ± 0.0003	0.158 ± 0.015	0.29 ± 0.03	0.12 ± 0.03
0.10-1.0	0.42 ± 0.05	0.039 ± 0.0005	0.218 ± 0.019	0.46 ± 0.05	0.23 ± 0.04
0.05-1.0	0.55 ± 0.06	0.057 ± 0.0007	0.368 ± 0.019	0.63 ± 0.06	0.25 ± 0.07
0.02-1.0	1.02 ± 0.10	0.086 ± 0.0009	0.555 ± 0.035	1.17 ± 0.10	0.60 ± 0.12
0.01-1.0	1.45 ± 0.12	0.114 ± 0.0010	0.655 ± 0.023	1.63 ± 0.12	0.88 ± 0.13

as large as the mass of the host galaxies (i.e. $\sim 10^{11} M_{\odot}$). The error bars in Fig. 5 are estimated using the contribution of Poisson errors based on the number of observed satellites and the standard deviation of the average number of fake satellites found in the simulations.

4.4 The merging channel of massive galaxies

Using the previous distribution of satellites, we can speculate about the stellar mass which could be potentially transferred to the hosts due to satellite infall. Under the assumption that eventually, all the satellites surrounding our massive galaxies will infall into their massive hosts, we can estimate which satellites could, in the future, contribute most to a potential mass growth of the host galaxy. On what follows, we assume that all satellites, independently of their mass, will infall with the same speed on the central galaxy. Note, however, that this could be not necessary true, since it is theoretically expected that most massive satellites will have shorter merging time-scale (e.g. Jiang et al. 2014).

To probe the most likely merger channel what we have done is the following. We have added all the stellar mass contained by the satellites within the intervals of stellar mass studied, then, we

divide this quantity by the sum of the mass of all the host galaxies, such as it indicates the following equation:

$$\Psi = \frac{\sum_{i=1}^{N_{\text{Sat-bin}}} M_{\text{Sat-bin},i}}{\sum_{j=1}^{N_{\text{Host}}} M_{\text{Host},j}} \quad (7)$$

The sum of all the mass in the host galaxies is a fixed quantity for our samples of hosts and their values are $\sum_{j=1}^{N_{\text{Host}}} M_{\text{Host},j} = (11.2, 5.26, 10.4, 6.76) \times 10^{12} M_{\odot}$ for (E, S0, Sa, Sb/c) types, respectively. These numbers correspond to the following typical masses per galaxy host: $\sum_{j=1}^{N_{\text{Host}}} M_{\text{Host},j} / N_{\text{Host}} = (1.3, 1.4, 1.3, 1.3) \times 10^{11} M_{\odot}$.

Our results are illustrated in Fig. 6 and Table 3 for each host sample, once corrected by the effects of background and clustering. Fig. 6 highlights the different way the stellar mass around the massive galaxies builds up as a function of the morphological type. The merger channel is mainly produced by satellites down to 1:10 for all the host samples. The average total amount of stellar mass contained in the satellite population down to 1:10 compared to the total amount of stellar mass in the hosts to the different morphological types studied is 45.4 ± 6.6 , 24.7 ± 7.5 , 14.3 ± 3.8 , 10.8 ± 3.7 per cent for E, S0, Sa, Sb/c types, respectively. Down to 1:100 these values increase up to 54.5 ± 15.1 , 30.5 ± 8.7 , 16.9 ± 4.3 , 12.6 ± 4.5 per cent of

Table 2. Differential number of satellites per host galaxy using the background ($N_{\text{Sat,S}}/N_{\text{Host}}$) and clustering corrections ($N_{\text{Sat,C}}/N_{\text{Host}}$) within a radial distance of 300 kpc and down to a mass ratio satellite–host 1:100. $N_{\text{Obs}}/N_{\text{Host}}$ is the observed number of satellites per host. $N_{\text{S}}/N_{\text{Host}}$ is the number of satellites per host in our background simulation and $N_{\text{C}}/N_{\text{Host}}$ the number of satellites per host within 500-600 kpc in our clustering analysis. The background and clustering corrections are derived independently for each morphological type as it is shown in the table.

$M_{\text{Sat}}/M_{\text{Host}}$	$N_{\text{Obs}}/N_{\text{Host}}$	$N_{\text{S}}/N_{\text{Host}}$	$N_{\text{C}}/N_{\text{Host}}$	$N_{\text{Sat,S}}/N_{\text{Host}}$	$N_{\text{Sat,C}}/N_{\text{Host}}$
E					
0.50-1.00	0.40 ± 0.03	0.006 ± 0.0001	0.080 ± 0.008	0.36 ± 0.03	0.29 ± 0.03
0.20-0.50	0.83 ± 0.03	0.015 ± 0.0002	0.251 ± 0.022	0.83 ± 0.03	0.59 ± 0.03
0.10-0.20	0.78 ± 0.03	0.017 ± 0.0002	0.322 ± 0.032	0.83 ± 0.03	0.52 ± 0.03
0.05-0.10	1.13 ± 0.03	0.018 ± 0.0002	0.338 ± 0.020	1.07 ± 0.03	0.77 ± 0.02
0.02-0.05	1.36 ± 0.05	0.029 ± 0.0003	0.389 ± 0.026	1.30 ± 0.05	0.93 ± 0.04
0.01-0.02	0.94 ± 0.02	0.028 ± 0.0003	0.467 ± 0.027	1.01 ± 0.02	0.58 ± 0.04
S0					
0.50-1.00	0.23 ± 0.02	0.005 ± 0.0001	0.032 ± 0.010	0.24 ± 0.02	0.21 ± 0.02
0.20-0.50	0.41 ± 0.03	0.014 ± 0.0002	0.137 ± 0.013	0.39 ± 0.03	0.26 ± 0.04
0.10-0.20	0.30 ± 0.03	0.017 ± 0.0003	0.174 ± 0.018	0.32 ± 0.03	0.16 ± 0.02
0.05-0.10	0.46 ± 0.04	0.019 ± 0.0003	0.005 ± 0.003	0.53 ± 0.04	0.50 ± 0.04
0.02-0.05	0.91 ± 0.05	0.028 ± 0.0004	0.255 ± 0.021	0.92 ± 0.05	0.68 ± 0.08
0.01-0.02	0.63 ± 0.04	0.029 ± 0.0004	0.141 ± 0.016	0.71 ± 0.04	0.50 ± 0.03
Sa					
0.50-1.00	0.11 ± 0.01	0.006 ± 0.0001	0.017 ± 0.003	0.12 ± 0.01	0.11 ± 0.01
0.20-0.50	0.27 ± 0.02	0.016 ± 0.0002	0.147 ± 0.014	0.27 ± 0.02	0.12 ± 0.01
0.10-0.20	0.29 ± 0.02	0.017 ± 0.0002	0.137 ± 0.023	0.27 ± 0.02	0.15 ± 0.03
0.05-0.10	0.30 ± 0.02	0.018 ± 0.0001	0.048 ± 0.009	0.31 ± 0.02	0.26 ± 0.02
0.02-0.05	0.57 ± 0.03	0.029 ± 0.0002	0.143 ± 0.017	0.54 ± 0.03	0.41 ± 0.03
0.01-0.02	0.40 ± 0.02	0.029 ± 0.0002	0.156 ± 0.014	0.36 ± 0.02	0.21 ± 0.02
Sb/c					
0.50-1.00	0.13 ± 0.03	0.006 ± 0.0001	0.041 ± 0.008	0.15 ± 0.03	0.10 ± 0.03
0.20-0.50	0.13 ± 0.01	0.016 ± 0.0002	0.125 ± 0.014	0.13 ± 0.01	0.02 ± 0.01
0.10-0.20	0.14 ± 0.02	0.017 ± 0.0003	0.046 ± 0.009	0.17 ± 0.02	0.12 ± 0.01
0.05-0.10	0.15 ± 0.02	0.019 ± 0.0002	0.150 ± 0.015	0.17 ± 0.02	0.02 ± 0.04
0.02-0.05	0.51 ± 0.06	0.028 ± 0.0002	0.186 ± 0.020	0.54 ± 0.06	0.35 ± 0.05
0.01-0.02	0.43 ± 0.03	0.028 ± 0.0002	0.153 ± 0.016	0.46 ± 0.03	0.29 ± 0.03

the total amount of mass contained in their hosts. These numbers indicate that the contribution of the low mass population of satellites 1:10-1:100 to the host mass is not significant compared to the mass ratio 1:1-1:10. We have assumed Poisson errors to estimate our error bars in the Fig. 6.

At limiting our exploration up to 100 kpc, the above results decrease notably. The satellites more massive than 1:10 are again the dominant mass contributor. The percentage which reflects that contribution with respect to the total mass of the hosts is roughly 14.6 ± 3.2 , 2.4 ± 1.3 , 7.9 ± 1.0 , 3.0 ± 2.1 per cent for E, S0, Sa, Sb/c types, respectively, corresponding to the mean of background-clustering results once applied the corrections. Down to 1:100, these percentages increase up to 17.2 ± 3.9 , 4.5 ± 2.1 , 8.7 ± 2.8 , 3.6 ± 2.4 .

As we pointed out before, if the satellites eventually infall into the host galaxies, the merger channel will be largely dominated by satellites with a mass ratio below 1:10 for all morphological types. For satellites up to 300 kpc (100 kpc), this corresponds to 67.2, 68.4, 88.1 and 85.7 (85, 57, 91 and 83) per cent of the total mass enclosed by the satellites within that radial distance. The contribution of the most massive satellites is particularly important for spiral types, and slightly weaker for early types. Down to 1:10, the distribution of stellar mass of the satellites reveals that the massive

E galaxies could have their main contributor between the relative masses 1:5-1:1 whereas the main contributor of the S0, Sa and Sb/c types is the most massive satellites (1:2-1:1). It is also worth noticing that elliptical galaxies can have up to ~ 4 times more mass in satellites of 1:10-1:100 compared to Sb/c types.

If the theoretical expectations are correct, and the merger time-scales are shorter for the most massive satellites, this mass growth due to the larger satellites will be even more important than the result shown in Fig. 6.

5 DISCUSSION

The results presented in this paper attempt to establish a robust $z \sim 0$ reference for the study of the evolution of the abundance of satellites around massive galaxies with cosmic time and their dependence with host morphology. In addition, it extends the results obtained in our previous work, Ruiz, Trujillo & Marmol-Queralto (2014), in which we studied the abundance of satellites around E-type hosts using the SDSS Data Release 7 (DR7). In this paper, we have completed that results, using a deeper spectroscopic sample and studying the satellite abundances also according to their host morphology.

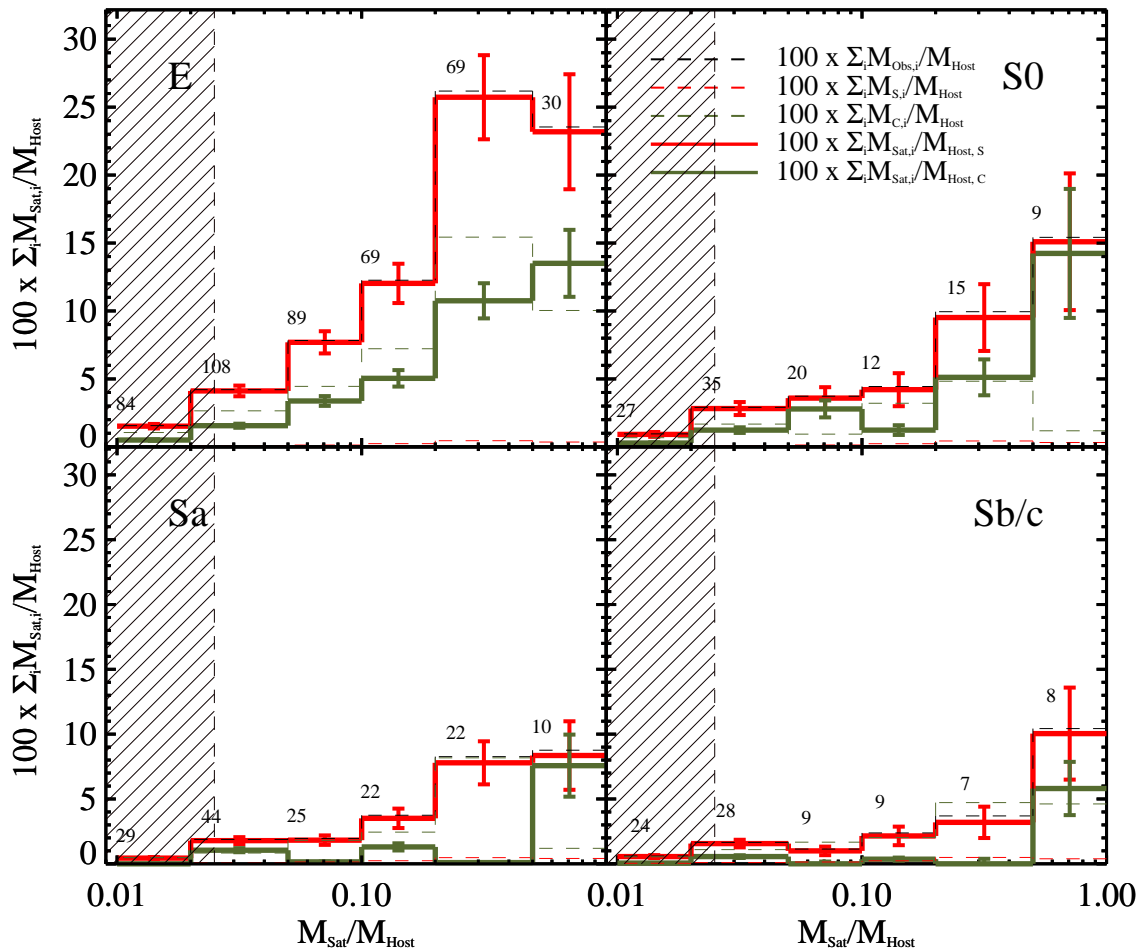


Figure 6. The merging channel of the massive galaxies as a function of their morphology. The panels show the contribution (in percentage) of the satellite mass enclosed in each mass bin to the total mass confined by their hosts for each morphological type. The red solid line represents this quantity after correcting for the background contaminant (Ψ_S), and the green solid line after correcting by clustering (Ψ_C). The black, red and green dashed lines show Ψ_{Obs} , Ψ_{Sim} and Ψ_{Clu} found in the observations, background simulations and clustering, respectively. The numbers over each bin correspond to the number of observed satellites within each mass interval. The vertical dashed area illustrates the region where the satellite incompleteness could play a role.

We have found that the abundance of satellites turns out to be significantly dependent on the morphology of the hosts for galaxies with similar stellar masses. The abundance of satellites is much higher around elliptical galaxies. The fact that Sb/c galaxies have fewer satellites around them probably helps to explain how they have maintained their disc-like structure during their lifetime. On the contrary, the large number of satellites around massive ellipticals could help to clarify the characteristic large envelopes surrounding these objects that are thought to be connected with intensive accretion.

Several works have recently estimated the number of satellites in different redshift intervals around massive galaxies both observationally and theoretically (see e.g. Chen 2008; Moster et al. 2010; Guo et al. 2011b, 2013; Lares et al. 2011; Liu et al. 2011; Nierenberg et al. 2012; Quilis & Trujillo 2012; Tal et al. 2012; Wang & White 2012; ?). The observational studies agree within the measurement uncertainties. However, the satellites in the simulations are, in general, more abundant. Some of these previous studies have shown that the number of satellites around massive galaxies of a given mass ratio has remained constant since at least

$z \sim 2$ (Jackson et al. 2010; Nierenberg et al. 2011, 2013; Man et al. 2012; Marmol-Queralto et al. 2012, 2013; Newman et al. 2012; Quilis & Trujillo 2012; Huertas-Company et al. 2013; Ferreras et al. 2014). In this paper, less affected by incompleteness at low stellar mass than previous works, we readdress this question and explore how the theoretical expectations compare to the observational data in the local Universe. We do this for our four different morphological types.

5.1 Abundance of satellites: comparison with previous works

5.1.1 Observations

In order to check the agreement of our results with the literature, we do a direct comparison with the abundance of satellites found by Wang & White (2012). In their work, the authors studied the number of satellites around a large sample of isolated massive galaxies to probe the Λ CDM scenario. In their paper, they segregated the massive galaxies not using visual morphology but

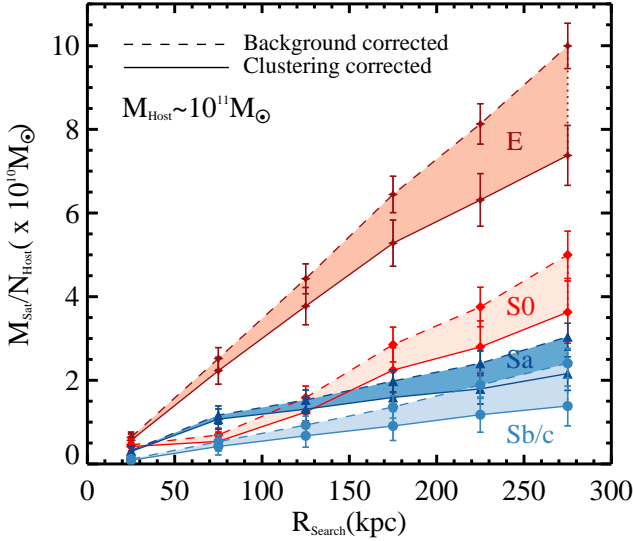


Figure 5. Cumulative stellar mass enclosed by satellites down to 1:100 as a function of the projected radial distance up to 300 kpc. The background contaminant correction, as well as the clustering correction, is applied for all the morphological types. The dark red lines correspond to centrals E, red S0, dark blue Sa and soft blue Sb/c type.

colours, and estimated the abundance of satellites according to the stellar mass of the satellites instead of the mass ratio satellite–host.

To make a direct comparison with Wang & White (2012), we also estimate the abundance of satellites according to the stellar mass instead the mass ratio satellite–host such as Wang & White (2012) did. Given that the average stellar mass of our host sample is $\log(M_*/M_\odot) \sim 11.1$, we have compared our numbers with the average value they get combining their results from the host mass bins $10.8 < \log(M_*/M_\odot) < 11.1$ and $11.1 < \log(M_*/M_\odot) < 11.4$ (their green and blue lines, respectively, in their figs 7 and 8). We confront our results for E and S0 types with the ones they found for their red hosts. Additionally, we explore the difference between the abundance of satellites in their blue hosts with our sample of disc galaxies (Sa and Sb/c types). Thus, we obtain, for satellites with $\log(M_*/M_\odot) = 10$, $N_{\text{Sat}}/N_{\text{Host}} = 0.31\text{--}0.44$ (ours) and $0.14\text{--}0.19$ (Wang & White) and, for satellites with $\log(M_*/M_\odot) = 9.0$, $N_{\text{Sat}}/N_{\text{Host}} = 0.50\text{--}0.65$ (ours) and $0.44\text{--}0.55$ (Wang & White). When we compare our disc types with their blue massive galaxies we find, for satellites with $\log(M_*/M_\odot) = 10$, $N_{\text{Sat}}/N_{\text{Host}} = 0.05\text{--}0.1$ (ours) and $0.07\text{--}0.12$ (Wang & White) and, for satellites with $\log(M_*/M_\odot) = 9.0$, $N_{\text{Sat}}/N_{\text{Host}} = 0.22\text{--}0.29$ (ours) and $0.08\text{--}0.15$ (Wang & White). Our results are significantly larger at comparing their red primaries with our early-type galaxies for $\log(M_*/M_\odot) = 10$ and closer for less massive satellites ($\log(M_*/M_\odot) = 9$). This trend is not reproduced in the comparison of blue primaries versus late-type galaxies where we find a closer agreement.

The difference with Wang & White (2012) is even larger if we consider a more extreme comparison: our massive elliptical galaxies versus their red primaries. In this case, we obtain for satellites with $\log(M_*/M_\odot) = 10$, $N_{\text{Sat}}/N_{\text{Host}} = 0.41\text{--}0.61$ (ours) and $0.14\text{--}0.19$ (Wang & White) and, for satellites with $\log(M_*/M_\odot) = 9.0$, $N_{\text{Sat}}/N_{\text{Host}} = 0.53\text{--}0.78$ (ours) and $0.44\text{--}0.55$ (Wang & White). This highlights the importance of morphology when we study the number of satellites. Several reasons can contribute to the differences found at comparing the red massive galaxies of Wang & White

Table 3. The merging channel of local massive galaxies for each morphological type. The table shows the contribution (in per cent) of the stellar mass enclosed in each satellite mass bin to the total mass confined by their hosts. We show the observed fraction (in per cent) Ψ_{Obs} as well as their values once corrected from background $\Psi_{\text{Sat,S}}$ and clustering $\Psi_{\text{Sat,C}}$.

$M_{\text{Sat}}/M_{\text{Host}}$	Ψ_{Obs} (per cent)	$\Psi_{\text{Sat,S}}$ (per cent)	$\Psi_{\text{Sat,C}}$ (per cent)
E			
0.50-1.00	23.54 ± 4.30	23.19 ± 4.23	13.50 ± 2.47
0.20-0.50	26.18 ± 3.15	25.73 ± 3.10	10.75 ± 1.29
0.10-0.20	12.26 ± 1.48	12.03 ± 1.45	5.04 ± 0.61
0.05-0.10	7.82 ± 0.83	7.69 ± 0.82	3.38 ± 0.36
0.02-0.05	4.21 ± 0.40	4.12 ± 0.40	1.56 ± 0.15
0.01-0.02	1.56 ± 0.17	1.52 ± 0.17	0.50 ± 0.06
Total	75.58 ± 10.33	74.27 ± 10.16	34.73 ± 4.93
S0			
0.50-1.00	15.42 ± 5.14	15.09 ± 5.03	14.23 ± 4.74
0.20-0.50	9.95 ± 2.57	9.51 ± 2.46	5.12 ± 1.32
0.10-0.20	4.44 ± 1.28	4.21 ± 1.21	1.23 ± 0.36
0.05-0.10	3.73 ± 0.83	3.59 ± 0.80	2.79 ± 0.62
0.02-0.05	2.91 ± 0.49	2.82 ± 0.48	1.23 ± 0.21
0.01-0.02	0.96 ± 0.18	0.92 ± 0.18	0.28 ± 0.05
Total	37.40 ± 10.50	36.14 ± 10.16	24.89 ± 7.31
Sa			
0.50-1.00	8.76 ± 2.77	8.35 ± 2.64	7.57 ± 2.39
0.20-0.50	8.26 ± 1.76	7.79 ± 1.66	0.09 ± 0.02
0.10-0.20	3.75 ± 0.80	3.51 ± 0.75	1.30 ± 0.28
0.05-0.10	1.96 ± 0.39	1.83 ± 0.37	0.15 ± 0.03
0.02-0.05	1.88 ± 0.28	1.79 ± 0.27	1.05 ± 0.16
0.01-0.02	0.48 ± 0.09	0.44 ± 0.08	0.00 ± 0.01
Total	25.09 ± 6.10	23.70 ± 5.77	10.17 ± 2.88
Sb/c			
0.50-1.00	10.43 ± 3.69	10.04 ± 3.55	5.81 ± 2.05
0.20-0.50	3.69 ± 1.40	3.20 ± 1.21	0.00 ± 0.39
0.10-0.20	2.38 ± 0.79	2.15 ± 0.72	0.36 ± 0.12
0.05-0.10	1.14 ± 0.38	1.00 ± 0.33	0.00 ± 0.18
0.02-0.05	1.65 ± 0.31	1.56 ± 0.30	0.56 ± 0.11
0.01-0.02	0.60 ± 0.12	0.56 ± 0.11	0.06 ± 0.01
Total	19.89 ± 6.69	18.51 ± 6.22	6.78 ± 2.86

(2012) with our early-type galaxies. The most important is probably the environment where the samples are immersed since their study focus only on isolated galaxies whereas we use all the galaxies. However, the abundance of satellites is some closer at extending the comparison to the poorer mass satellites. This is likely due to our incompleteness around $10^9 M_\odot$. In contrast, this effect is not so evident at comparing blue-massive versus our late-type galaxies since these galaxies more likely live in less crowded environment.

From the above results we highlight two different characteristics. First, the isolation criteria used in previous works probably biases the global distribution of satellites around the massive galaxies. And second, the determination of abundance of satellites using morphological criteria enhances the differences in the number of satellites compared those based on segregating the samples simply by colour. This implies a stronger connection between the galaxy morphology and their number of satellites larger than a potential connection between the satellites and the stellar population of their hosts.

We can also compare our results with the recent work by Ruiz, Trujillo & Mármol-Queraltó (2014) on the satellite populations around massive elliptical galaxies in the local universe. In that work, we studied the abundance of satellites within a radial

distance of 100 kpc and selected the host samples within the redshift range 0.02-0.065. We found, after applying the contamination corrections, that $N_{\text{Sat}}/N_{\text{Host}}$ was between 0.24 and 0.28 for satellites up to 1:10 using a spectroscopic catalogue and $N_{\text{Sat}}/N_{\text{Host}}$ 0.84 and 0.98 when we extended our search up to 1:100 using a catalogue of photometric redshifts ('photo-z'; SDSS DR7). In our new host sample of massive ellipticals, we obtain higher values for both ratios (0.36-0.43 for 1:10 and 1.12-1.31 for 1:100) when we restrict our search radius down to $R=100$ kpc. The difference between the average stellar mass of both samples is 0.1 dex, being the average of Ruiz, Trujillo & Marmol-Queralto (2014)'s sample larger. This difference then could be attributed to technical characteristics as the effect of the 'tiling' of SDSS at different redshifts. In fact, in our previous work, we estimated that we could approximately lose up to 25 per cent of our potential satellites due to fibre collisions, a quantity which could partially explain that difference in the case 1:10. Also, it could be playing a role the samples selected in both works. In fact, the selection of E galaxies done in Ruiz, Trujillo & Marmol-Queralto (2014) is based on Nair & Abraham (2010) whereas the present classification is based on our own morphological analysis. Being the galaxies in the present sample significantly closer than those in Ruiz, Trujillo & Marmol-Queralto (2014), our ability to distinguish among E and S0 could be higher. In this sense, it worth stressing that the abundance of satellites found around S0 massive galaxies for 1:10 and 1:100 is 0.12-0.15 and 0.68-0.72, respectively. If we combine the E and S0 results, for 1:10, we get ~ 0.24 -0.29 and 0.9-1.05 for 1:100. This is also in good agreement with our previous results (Ruiz, Trujillo & Marmol-Queralto 2014).

Leaving aside the number of satellites found per host, we can now draw our attention to the fraction of massive galaxies with satellites found in other works at $z=0$, a parameter easily evaluable from our study. In this context, Liu et al. (2011), exploring Milky Way-like galaxies, found that only 12 per cent of those objects have at least a satellite within $R=100$ kpc down to 1:10 mass ratio (private communication). We have evaluated the fraction of massive host having satellites down to 1:10 in our disc-like hosts. We find 10-12 per cent once corrected from clustering and background contaminant. At segregating between the Sa and Sb/c samples, that fraction is 0.15 and 0.07, respectively. Our results are in good agreement with Liu et al. (2011).

Also, we can make a comparison with Marmol-Queralto et al. (2012). In this work, the authors conducted a similar analysis to what we have done here but for galaxies at higher redshifts ($0.2 < z < 2$). We compare our numbers with the galaxies they classified as spheroids in their lower redshift range ($0.2 < z < 0.75$). They found that the fraction of massive galaxies with satellites around the sample and down to 1:10 is 23-28 per cent. Our results for spheroids, E and S0 massive galaxies, are approximately 28 and 34 per cent, respectively. As we commented before, this comparison depends largely on the classification or grouping of the massive galaxies. A sample of spheroids with many S0 objects reduces the satellite abundance whereas a higher purity in the E-type sample increases it. We can also compare with the galaxies they classified as disc-like in the same redshift range, they find that the fraction of massive galaxies with at least a satellite was 5-9 per cent. A closer but lower value to our disc-like 10-13 per cent. However, as we mentioned before, at splitting into the morphological types Sa and Sb/c (we obtained 15 and 7 per cent, respectively) the agreement could depend again on the number of members of each morphological type.

Other works by Chen (2008), Guo et al. (2011b),

Nierenberg et al. (2012) or Kawinwanichakij et al. (2014) also searched for satellites around massive galaxies segregating their samples by colours, early- and late-type morphologies or even quiescent and star-forming galaxies. Some of the results of these works can be compared with our results due to the similarity in the satellite search criteria. Nevertheless, these authors computed the potential satellites as a function of the visual or r -band magnitude contrast satellite-host (Chen 2008; Guo et al. 2011b; Nierenberg et al. 2012) instead the mass ratio. Therefore, in order to compare with them, we also made our search for satellites using the r -band contrast magnitude between the satellite and its host.

In Guo et al. (2011b), the authors studied the luminosity function of satellite galaxies around isolated bright hosts ($M_r \sim -21.25$) using SDSS galaxy samples. They scaled their search radius to 300 kpc and found that the average number of satellites per host was 0.1 for red hosts and 0.06 for blue hosts when they studied satellites for $\Delta m_r \sim 2.5$ (see their fig.9). In addition, they split their sample into early and late types, finding similar results. At comparing with their late or blue hosts, the results are far from our abundance of satellites using that r -band magnitude contrast, we obtain $N_{\text{Sat}}/N_{\text{Host}} \sim 0.15$ -0.21. Also, when we compare with our results for early-type galaxies, we obtain $N_{\text{Sat}}/N_{\text{Host}} \sim 0.41$ -0.60, an amount significantly higher than those of Guo et al. (2011b). A possible explanation to this difference could be linked to their stellar mass distribution. To build their fig.9 they use host galaxies within the magnitude range $-20.75 < M_r < -21.75$ whereas our host sample is around $-21.5 < M_r < -22.5$.

Interestingly, Chen (2008) also studied the satellites around bright isolated galaxies, but unlike Guo et al. (2011b), the authors chose their host sample in the nearby Universe ($z < 0.045$). That sample was somewhat brighter than Guo et al. (2011b)'s one ($-20 < M_r < -23$) and they used a mildly shallower sample of satellites ($\Delta m_r < 2$). Under these conditions, they found an abundance of satellites per host of 0.3-0.4 and ~ 1.0 for blue and red hosts, respectively. This abundance of satellites found by Chen (2008) is some lower than our results for Sa and Sb/c types combined 0.42-0.60 for $\Delta m_r < 2$ but close to our results around the Sb/c types (0.37-0.53) considering our clustering correction. Also, our abundance of satellites for (E, S0) hosts combined (1.31-1.79) is larger than which Chen (2008) found. This likely due to the isolation criteria applied to select their host sample.

As we have seen above, there are multiple factors which affect to comparison with other works. The usage of colours or morphology for selecting the hosts, the search criteria for satellites, the difference among the stellar mass distributions of confronted samples or the density of galaxies where these samples are immersed. Nonetheless and in general, we get a reasonable agreement with the literature when we compare galaxies with disc like morphologies, our Sa and Sb/c types. As we mentioned before, these massive galaxies are thought to live in less crowded environments and therefore, their abundance of satellites should not be susceptible to change too much at applying them an isolation criterion unlike what happens with early-type hosts and mainly with the massive ellipticals. The majority of works showed above have used host samples using an isolation criterion. This probably biases the global distribution of satellites since it does not consider the excess of satellites linked to crowded regions in the real Universe. Precisely, in these comparisons, our abundance of satellites around early-type galaxies is, typically, larger, especially considering our sample of massive ellipticals. In fact, this excess is softened due to the mixture of E and S0 galaxies (Ruiz, Trujillo & Marmol-Queralto 2014) since

the S0 massive galaxies are typically in similar environments than the Sa types.

In that sense, a recent study by Guo et al. (2015) investigated the dependence of the luminosity function of the host galaxies as a function of inhabiting a filament or not using the SDSS data set. They found that the filamentary environment can increase the abundance of the brightest satellites by a factor of ~ 2 compared with non-filament isolated galaxies. This can help to explain the discrepancy with other observational works which used isolation (e.g. Chen 2008; Guo et al. 2011b; Wang & White 2012) since many of our massive elliptical galaxies are expected to be in dense regions.

5.1.2 Theory

Quilis & Trujillo (2012) estimated, using the Millennium Simulations, the expected fraction of massive galaxies with satellites with a mass ratio down to 1:10 and down to 1:100 within a sphere of $R = 100$ kpc. They conducted their study exploring galaxies from $z=2$ to now using three different semi-analytical models (Bower et al. 2006; DeLucia et al. 2007; Guo et al. 2011a). At $z=0$, the theoretical expectations suggested that the fraction of massive galaxies with at least a satellite down to 1:10 ranges from 0.3 to 0.4 and down to 1:100 from 0.6 to 0.7. We have studied that fraction in our work once applied the clustering corrections. E type (0.28, 0.63), S0 type (0.10, 0.39), Sa type (0.14, 0.35), Sb/c type (0.06, 0.20) for 1:10 and 1:100, respectively. For the full sample of massive galaxies, we get 0.14 studying satellites up to 1:10 and 0.39 down to 1:100. Summarizing, the theory makes a good prediction if we compare their numbers with massive ellipticals but it obtains an important over-prediction of satellites when we extend the host sample to all our host galaxies.

It is worth stressing that this discrepancy among the theoretical and the observational results can not be explained due to the different volumes of exploration used in both works: a spatial sphere of 100 kpc in Quilis & Trujillo (2012) and a cylinder in redshift here. Because the way we have selected our galaxies in redshift, basically all the satellites in the line of sight of the host within a projected radial distance up to 100 kpc are taken. In that sense, at comparing with the Millennium Simulation our number of observed satellites should be an upper limit (as they are only restricted to 100 kpc in depth). As the number of theoretical satellites is larger than observed, we can confidently claim that there is a discrepancy with our observations. Finally, a potential loss of satellites in the work by Quilis & Trujillo (2012) due to resolution effects will also increase the discrepancy between the simulations and the observations.

In this same theoretical context, we find the work of Guo et al. (2013) who investigated the luminosity functions of galactic satellites around isolated bright hosts from model satellites placed into the Millennium and Millennium II dark matter simulations by the GALFORM semi-analytic galaxy formation model. These luminosity functions allow us to compare with our results. In their work, Guo et al. (2013) used bright hosts within the range $-21.5 < M_r < -22.5$ and the same search radius than us. They found that the number of satellites per host was 0.29 and 0.07 (see the upper panel of their fig.8) segregating their sample in red and blue hosts for $\Delta m_r \sim 2.5$, respectively. Around this value, we find that the abundance of satellites is 0.15-0.21 for (Sa, Sb/c) galaxies. Our number of satellites per red host is also much larger than the found by Guo et al. (2013). We obtain 0.41-0.60 for $\Delta m_r \sim 2.5$. For less brighter satellites, $\Delta m_r \sim 4$, Guo et al. (2013) obtain for red and blue hosts 0.5 and 0.11, respectively, whereas we obtain the ranges

0.40-0.72 and 0.18-0.29 for (E, S0) and (Sa, Sb/c), respectively. The abundance of satellites for our blue hosts remains a factor of 2 larger whereas the number of satellites found by Guo et al. (2013) increase significantly to reach a similar amount to ours. In their work, Guo et al. (2013) also compared with observational results from SDSS DR8. Despite having found a good agreement between observations and models for red primaries, they found dramatic differences around blue primaries, placing the model a factor of 2-3 fewer satellites than are present around comparable SDSS primaries.

5.2 Mass and efficiency of the dark matter haloes

Assuming that there is a link between the dark matter halo mass and the number of satellites a galaxy has (Wang & White 2012; ?; Kawinwanichakij et al. 2014), we can speculate how the relative abundance of satellites found in our different morphological samples are related to their halo masses. For example, if we compare the combined abundance of satellites around E and S0 types down to 1:100, with the number of satellites per host around Sb/c massive galaxies (grouping early versus late type), we obtain a factor of 3 higher in the number of satellites around early-type galaxies than late types. This implies that on average, the dark matter halo mass of early massive galaxies could be three times larger than the halo masses associated with our Sb/c galaxies. We assume here that the number of satellites is approximately proportional to the dark matter halo mass (Wang & White 2012; ?). Wang & White (2012) also studied that difference using massive galaxies ($\log(M_*/M_\odot) \sim 11.2$). In their work, they found that the red centrals had about a factor of 2 more satellites than blue centrals.

Interestingly, Mandelbaum et al. (2006) estimated the efficiency with which baryons in the halo of the galaxies have been converted into stars using a large sample of weak gravitational lenses ($0.02 < z < 0.3$), finding that the relative efficiency between late- and early-type galaxies with stellar masses (see their table 3) between $\log(M_*/M_\odot) \sim 11.0$ and 11.3 (the mean stellar mass of our samples is $\log(M_*/M_\odot) \sim 11.11$) was 2.5-4.36. If we consider a similar stellar mass for our samples and using the Equation 7 of Mandelbaum et al. (2006), we can compare our relative conversion efficiency. That range of relative efficiency between late and early types is, considering our background and clustering corrections, 2.6 and 2.9, a value in good agreement with their results. Following the above discussion, we can claim that the haloes of early-type massive galaxies are typically 2-3 times less efficient to convert the baryons into stars than the haloes of late-type massive galaxies. A factor which rises, in our more extreme comparison, to 3-4 at comparing the sample of ellipticals and the Sb/c types. At extending that relative efficiency in the terms explained before, to other morphological types, we find that our massive late spirals (Sa) are 15-43 per cent less efficient than the Sb/c ones. Within early-type ones, the massive lenticulars are a 58-74 per cent more efficient producing stars than ellipticals ones.

It is also interesting to compare with the statistical approach carried out by Moster et al. (2010) to determine the relationship between the stellar masses of galaxies and the masses of the dark matter haloes in which they reside. In their work, they estimated the average number of satellites as a function of the dark matter halo mass using a halo occupation model. The mean number of satellites is illustrated in their central panel of their fig.10. Under the assumption that down to 300 kpc we are taking all the satellites around our massive galaxies and, considering that our completeness is around $\log(M/M_\odot) \sim 9.0$ (pointed line in their fig.10), we could

do a direct comparison to establish the typical halo mass associated with each one of our samples using the abundance of satellites obtained after the corrections of background and clustering. We obtain for E-type massive galaxies a halo mass $M_{\text{Halo}} \sim 8.5\text{--}14.9 \times 10^{12} M_{\odot}$, for the S0 types $M_{\text{Halo}} \sim 5.4\text{--}7.2 \times 10^{12} M_{\odot}$, for the Sa types $M_{\text{Halo}} \sim 3.2\text{--}4.5 \times 10^{12} M_{\odot}$ and for Sb/c types a halo mass $M_{\text{Halo}} \sim 2.2\text{--}3.5 \times 10^{12} M_{\odot}$.

From these data, we can conduct other interesting estimation using the average stellar mass of our samples of massive galaxies and the equation (7) from Mandelbaum et al. (2006). This allows us to estimate again the conversion efficiency of baryons η obtained for the different morphological types E, S0, Sa and Sb/c starting from the Moster et al. (2010)'s results. We find 0.06-0.10, 0.13-0.17, 0.19-0.27 and 0.24-0.39, respectively. Interestingly, at combining (E,S0) and (Sa,Sb/c), grouping in early and late-types, we find a relative conversion efficiency of 2.3-2.4 between late and early-type galaxies. A factor close to the one already showed before when we compare that conversion efficiency with the Mandelbaum et al. (2006)'s work. In this context, More et al. (2011) find that the difference between halo mass of red and blue centrals is ~ 0.4 dex as the stellar mass of the central is $\log(M_{\star}/M_{\odot}) \sim 11.1$. This difference is also computed by Kawinwanichakij et al. (2014) and Phillips et al. (2014). They find a lower factor studying samples of quiescent and star-forming massive galaxies with $\log(M_{\star}/M_{\odot}) > 10.78$ ($1 < z < 3$) and $\log(M_{\star}/M_{\odot}) \sim 10.5$ (locally). Their samples of quiescent centrals have a higher median halo mass by a factor of ~ 0.3 dex (factor 2). This lower factor compared to our results and the previous results found in the literature could be produced by the combination of two factors, a lower mean stellar mass of the galaxies explored, and a larger difference among the halo masses of the samples studied in the nearby Universe respect to the halo masses of the galaxies in the redshift range window of Kawinwanichakij et al. (2014)'s sample.

Finally, Dutton et al. (2010) estimated the star formation efficiencies from satellite kinematics, weak gravitational lensing, and halo abundance matching at redshift $z \sim 0$. They found that the formation efficiency of early-type galaxies reached a peak of ~ 12 per cent at $M_{\star} \sim 10^{10.5} h^{-2} M_{\odot}$, decreasing to 2.8 per cent at $M_{\star} \sim 10^{11.4} h^{-2} M_{\odot}$. In contrast, this efficiency was between 26 and 33 per cent for late-type galaxies whose stellar mean mass estimated was $M_{\star} \sim 10^{11.0} h^{-2} M_{\odot}$. Both results are consistent with those ones showed before and therefore reinforce our hypothesis of proportionality between number of satellites and dark mass halo we assume as a starting point.

5.3 The main contributor to the growth of massive galaxies

There is growing consensus (see e.g. a discussion in Trujillo et al. 2011) that the size evolution can not be entirely explained by internal mechanisms like active galactic nuclei (AGN) activity (Fan et al. 2008, 2010; Ragone-Figueroa & Granato 2011). However, it is not clear what is the relevance of major versus minor merging in the growth of the galaxies. On one hand, major mergers (e.g. Ciotti & van Albada 2001; Nipoti, Londrillo, & Ciotti 2003; Boylan-Kolchin, Ma, & Quataert 2006; Naab et al. 2007) seem to be very scarce (at least since $z \sim 1$; Bundy et al. 2009; deRavel et al. 2009; Wild et al. 2009; López-Sanjuan et al. 2010; Kaviraj et al. 2011) to play a major role in the growth of the galaxies. On the other hand, minor merging (favoured theoretically for its efficiency on increasing the size of the galaxies; Khochfar & Burkert 2006; Maller et al. 2006; Hopkins et al. 2009b; Naab et al. 2009) con-

fronts some problems with the number of satellites found at $z \sim 1$ (e.g. Ferreras et al. 2014).

In order to investigate the physical origin of the observed strong increase in galaxy sizes since redshift $z \sim 2$, Oser et al. (2012) led a theoretical study in which they found that the evolution of massive early-type galaxies and their present-day properties are predominantly determined by frequent mergers of moderate mass (1:5) and not only by major mergers. Ferreras et al. (2014) probed the merging channel of massive galaxies ($M_{\star} \geq 10^{11} M_{\odot}$) over the $z=0.3\text{--}1.3$ redshift window and down to a mass ratio satellite-host 1:100, segregating their sample into early and late-type massive galaxies (see their fig.9). They found that the main contributor to the growth of the host mass is those satellites whose mass ratio satellite-host is $\sim 1:3$ for both samples.

We find at $z=0$ a merger channel dominated by satellites with mass ratio satellite-host larger than 1:5 for E-type massive galaxies, or dominated by satellites more massive than 1:2 if we consider our clustering correction as the most reliable. We find same result for the rest of morphological types, the most massive satellites are the main mass growth contributors. The growth of massive S0, Sa and Sb/c galaxies seems to be dominated by satellites more massive than 1:2. However, it is evident that massive ellipticals have a significant large number of satellites with masses ranging between 1:2 and 1:5. Concretely, and if we focus on our results after clustering correction, the contribution of these satellites is similar to the ones within the range 1:1-1:2. This is not seen in the rest of morphological types. The S0 types also show a non-negligible contribution to the host mass within the interval 1:2-1:5 but lower than a factor of 2 compared to the contribution of satellites of similar mass around ellipticals. In contrast, spiral types barely have satellites in this mass range. It is then interesting to study if this 1:2-1:5 merging channel remains growing when we assess the contribution of the satellites around a still more massive host sample of massive ellipticals and if it is reproduced at higher redshift. In this context, a better identification of massive ellipticals and lenticulars may be key to check whether this highlighted channel 1:2-1:5 also exists.

As the merger channel since $z \sim 1$ is similar to the one found here locally, the observations suggest that the mass and size increase of the elliptical massive galaxies will be dominated by satellites with mass ratio within 1:1-1:5 (see also López-Sanjuan et al. 2012; Ruiz, Trujillo & Marmol-Queraltó 2014) whereas other morphological types as S0, Sa and Sb/c seem to associate that increase to mergers with satellites with similar masses to the host. Note, however, that these statements assume that the merger time-scale are independent of the mass ratio between the satellites and the host galaxies. More realistic scenarios (e.g. Jiang et al. 2014) suggest that the merger time-scale rises as the mass ratio between both galaxies increases. Accordingly, the smaller satellites will take significantly more time to merge with the host galaxies than the more massive ones.

Based on this, what we can claim with some confidence is that low-mass satellites with mass ratio below 1:10 would play a minor role in the mass increase of the host galaxies. They would be just very small in number to contribute to the mass growth, plus they will have very large time-scales to efficiently infall into the massive galaxies. However, the small satellites could be playing a major role in the construction of the stellar haloes of the galaxies (see e.g. Cooper et al. 2013). If the theoretical expectation remains, and the merger time-scales are shorter for the most massive satellites, this mass growth due to the larger satellites will be even more important than the result showed in Fig. 6.

6 SUMMARY AND CONCLUSIONS

In this paper we explore the abundance of satellites around 254 massive ($10^{11} < M_{\star} < 2 \times 10^{11} M_{\odot}$) low- z ($z < 0.025$) galaxies visually classified as E, S0, Sa and Sb/c. Using the SDSS DR10 spectroscopic catalogue, the proximity of our host galaxies guarantees that we can explore satellites with completeness down to $M_{\star} \sim 10^9 M_{\odot}$. Our satellite galaxies have been identified within a projected radial distance of 300 kpc around the central galaxy. A careful statistical analysis of the background and clustering has been applied to decontaminate the number of satellites from fake satellites. The abundance of satellites decline significantly from the E galaxies to S0, Sa and Sb/c types showing an important dependence with the morphology of the host independently of the mass ratio satellite–host. The average number of satellites down to a mass ratio 1:100 within 300 kpc is 4.5 ± 0.3 for E hosts, 2.6 ± 0.2 for S0, 1.5 ± 0.1 for Sa and 1.2 ± 0.2 for Sb/c. These quantities decrease by a factor of 2.5-3.5 down to 1:10.

Under the assumption that there is a proportionality between the number of satellites found and the dark matter halo mass, we find that the haloes of massive ellipticals are less efficient than the haloes of Sb/c types on converting their baryons into stars by a factor of 3-4. We need a halo 3-4 times more massive to create an elliptical with the same stellar mass than a Sb/c spiral. This factor decreases to ~ 3 when we group our samples in early- and late-type massive galaxies.

If the satellites would eventually infall into their host galaxies, the growth of massive galaxies will be dominated by satellites with a mass ratio down to 1:10. Those satellites are the main contributors to the stellar mass enclosed by the satellites and responsible of the 67.2, 68.4, 88.1 and 85.7 per cent of the total mass in satellites for E, S0, Sa, and Sb/c types, respectively, down to 300 kpc. Massive ellipticals seem to be surrounded by a remarkably larger number of poor massive satellites whereas the rest of morphological types typically merge with more massive objects. Specifically, the main contributor to the growth of massive spirals seems to be the satellites more massive than 1:2 (to the S0, Sa and Sb/c types). To the E hosts, the merger channel peaks within 1:1-1:5, in agreement with the 1:5 pointed by Oser et al. (2012).

These results could be used in future works to test the Λ CDM predictions about the number of satellites surrounding the most massive galaxies in the present-day Universe according to their morphology. In addition, the results presented here show the most likely merging channel of present-day massive galaxies. Finally, our work highlights the importance of the environment where massive galaxies are immersed and how that environment is strongly linked to the host morphology.

ACKNOWLEDGEMENTS

We thank the referee for detailed and constructive revision of the manuscript. This work has been supported by the ‘Programa Nacional de Astronomía y Astrofísica’ of the Spanish Ministry of Science and Innovation under grant AYA2013-48226-C3-1-P. EM-Q acknowledges the support of a European Research Council Consolidator Grant (PI: McLure).

This project has made use of data from the Sloan Digital Sky Survey (SDSS). Funding for the SDSS has been provided by the Alfred P. Sloan Foundation, the Participating Institutions, the National Science Foundation, the US Department of Energy, the National Aeronautics and Space Administration, the Japanese

Monbukagakusho, the Max Planck Society and the Higher Education Funding Council for England. The SDSS web site is <http://www.sdss.org/>

The SDSS is managed by the Astrophysical Research Consortium for the Participating Institutions. The Participating Institutions are the American Museum of Natural History, Astrophysical Institute Potsdam, University of Basel, University of Cambridge, Case Western Reserve University, University of Chicago, Drexel University, Fermilab, the Institute for Advanced Study, the Japan Participation Group, Johns Hopkins University, the Joint Institute for Nuclear Astrophysics, the Kavli Institute for Particle Astrophysics and Cosmology, the Korean Scientist Group, the Chinese Academy of Sciences (LAMOST), Los Alamos National Laboratory, the Max-Planck-Institute for Astronomy (MPIA), the Max-Planck-Institute for Astrophysics (MPA), New Mexico State University, Ohio State University, University of Pittsburgh, University of Portsmouth, Princeton University, the United States Naval Observatory, and the University of Washington.

REFERENCES

- Ahn, C. P., et al. 2014, *ApJS*, 211, 17
 Bailin J., Power C., Norberg P., Zaritsky D., Gibson B. K., 2008, *MNRAS*, 390, 1133
 Bell E. F., McIntosh D. H., Katz N., Weinberg M. D., 2003, *ApJS*, 149, 289
 Bezanson R., van Dokkum P. G., Tal T., Marchesini D., Kriek M., Franx M., Coppi P., 2009, *ApJ*, 697, 1290
 Bournaud, F., et al., 2011, *ApJ*, 730, 4
 Bower, R. G., Benson, A. J., Malbon, R., Helly J. C., Frenk C. S., Baugh C. M., Cole S., Lacey C. G., 2006, *MNRAS*, 370, 645
 Boylan-Kolchin M., Ma C.-P., Quataert E., 2006, *MNRAS*, 369, 1081
 Buitrago F., Trujillo I., Conselice C. J., Bouwens R. J., Dickinson M., Yan H., 2008, *ApJL*, 687, L61
 Bundy K., Fukugita M., Ellis R. S., Targett T. A., Belli S., Kodama T., 2009, *ApJ*, 697, 1369
 Carrasco E. R., Conselice C. J., Trujillo I., 2010, *MNRAS*, 405, 2253
 Cenarro A. J., Trujillo I., 2009, *ApJ*, 696, L43
 Chen, J., 2008, *A&A*, 484, 347
 Chen J., Kravtsov A. V., Prada F., Sheldon E. S., Klypin A. A., Blanton M. R., Brinkmann J., Thakar A. R., 2006, *ApJ*, 647, 86
 Ciotti L., van Albada T. S., 2001, *ApJ*, 552, L13
 Cooper, A. P., D’Souza, R., Kauffmann, G., Wang J., Boylan-Kolchin M., Guo Q., Frenk C. S., White S. D. M., 2013, *MNRAS*, 434, 3348
 Dekel, A., et al., 2009, *Nature*, 457, 451
 DeLucia G., Blaizot J., 2007, *MNRAS*, 375, 2
 de Ravel L., et al., 2009, *A&A*, 498, 379
 Díaz-García, L. A., Mármol-Queraltó, E., Trujillo, I., Cenarro A. J., López-Sanjuan C., Pérez-González P. G., Barro G., 2013, *MNRAS*, 433, 60
 Dutton, A. A., Conroy, C., van den Bosch, F. C., Prada, F., & More, S. 2010, *MNRAS*, 407, 2
 Erwin, P., Pohlen, M., Gutiérrez, L., & Beckman, J. E. 2008, in Funes J. G., Corsini E. M., eds, *ASP Conf. Ser. Vol. 396, Formation and Evolution of Galaxy Disks*. Astron. Soc. Pac., San Francisco, p. 207
 Fan L., Lapi A., De Zotti G., Danese L., 2008, *ApJL*, 689, L101

- Fan L., Lapi A., Bressan A., Bernardi M., De Zotti G., Danese L., 2010, *ApJ*, 718, 1460
- Feldmann, R., Carollo, C. M., & Mayer, L. 2011, *ApJ*, 736, 88
- Ferreras, I., et al., 2014, *MNRAS*, 444, 906
- Fu, Y. N., Huang, J. H., & Deng, Z. G. 2003, *MNRAS*, 339, 442
- Guo Q., White S., et al., 2011a, *MNRAS*, 413, 101
- Guo, Q., Cole, S., Eke, V., & Frenk, C. 2011b, *MNRAS*, 417, 370
- Guo, Q., Cole, S., Eke, V., Frenk, C., & Helly, J., 2013, *MNRAS*, 434, 1838
- Guo, Q., Tempel, E., & Libeskind, N. I., 2015, *ApJ*, 800, 112
- Hernquist, L., & Barnes, J. E. 1991, *Nature*, 354, 210
- Hopkins, P. F., Bundy, K., Murray, N., Quataert E., Lauer T. R., Ma C.-P., 2009a, *MNRAS*, 398, 898
- Hopkins P. F., Hernquist L., Cox T. J., Keres D., Wuyts S., 2009b, *ApJ*, 691, 1424
- Huertas-Company M., Shankar F., Mei S., Bernardi M., Aguerri J. A. L., Meert A., Vikram V., 2013, *ApJ*, 779, 29
- Jackson, N., Bryan, S. E., Mao, S., & Li, C. 2010, *MNRAS*, 403, 826
- Jiang, C., Jing, Y., & Han, J., 2014, *ApJ*, 790, 7
- Kauffmann, G., et al., 2003, *MNRAS*, 341, 33
- Kaviraj S., Tan K.-M., Ellis R. S., Silk J., 2011, *MNRAS*, 411, 2148
- Kawinwanichakij, L., et al., 2014, *Apj*, 792, 103
- Kereš, D., Katz, N., Weinberg, D. H., & Davé, R. 2005, *MNRAS*, 363, 2
- Khochfar, S., & Silk, J. 2006, *ApJ*, 648, L21
- Khochfar S., Burkert A., 2006, *AJ*, 445, 403
- Kroupa P., 2001, *MNRAS*, 322, 231
- Kroupa, P., et al., 2010, *ApJ*, 523, A32
- Kroupa, P., 2012, *Publ. Atron. Soc. Aust.*, 29, 395
- Lares, M., Lambas, D. G., & Domínguez, M. J., 2011, *AJ*, 142, 13
- Liu L., Gerke B. F., Wechsler R. H., Behroozi P. S., Busha M. T., 2011, *ApJ*, 733, 62
- López-Sanjuan C., Ballcells M., Pérez-González P. G., Barro G., García-Dabó C. E., Gallego J., Zamorano J., 2010, *ApJ*, 710, 1170
- López-Sanjuan C., et al., 2012, *A&A*, 548, A7
- Maller A. H., Katz N., Kereš D., Davé R., Weinberg D. H., 2006, *ApJ*, 647, 763
- Man A. W. S., Toft S., Zirm A. W., Wuyts S., van der Wel A., 2012, *ApJ*, 744, 85
- Mandelbaum, R., Seljak, U., Kauffmann, G., Hirata, C. M., & Brinkmann, J. 2006, *MNRAS*, 368, 715
- Mármol-Queraltó, E., Trujillo, I., Pérez-González, P. G., Varela, J., & Barro, G., 2012, *MNRAS*, 422, 2187
- Mármol-Queraltó, E., Trujillo, I., Villar, V., Barro, G., & Pérez-González, P. G., 2013, *MNRAS*, 429, 792
- Montes, M., Trujillo, I., Prieto, M. A., & Acosta-Pulido, J. A., 2014, *MNRAS*, 439, 990
- More, S., van den Bosch, F. C., Cacciato, M., Skibba R., Mo H. J., Yang X., 2011, *MNRAS*, 410, 210
- Moster, B. P., Somerville, R. S., Maulbetsch, C., van den Bosch F. C., Macció A. V., Naab T., Oser L., 2010, *Apj*, 710, 903
- Naab T., Johansson P. H., Ostriker J. P., Efstathiou G., 2007, *ApJ*, 658, 710
- Naab T., Johansson P. H., Ostriker J. P., 2009, *ApJ*, 699, L178
- Nair P. B., Abraham R. G., 2010, *ApJS*, 186, 427
- Newman A. B., Ellis R. S., Bundy K., Treu T., 2012, *ApJ*, 746, 162
- Nierenberg, A. M., Auger M. W., Treu T., Marshall P. J., Fassnacht C. D., 2011, *ApJ*, 731, 44
- Nierenberg, A. M., Auger, M. W., Treu, T., Marshall P. J., Fassnacht C. D., Busha M. T., 2012, *ApJ*, 752, 99
- Nierenberg A. M., Treu T., Menci N., Lu Y., Wang W., 2013, *ApJ*, 772, 146
- Nipoti C., Londrillo P., Ciotti L., 2003, *MNRAS*, 342, 501
- Oser, L., Ostriker, J. P., Naab, T., Johansson, P. H., & Burkert, A. 2010, *ApJ*, 725, 2312
- Oser L., Naab T., Ostriker J. P., Johansson P. H., 2012, *ApJ*, 744, 63
- Padmanabhan, N., et al., 2008, *ApJ*, 674, 1217
- Phillips, J. I., Wheeler, C., Boylan-Kolchin, M., Bullock J. S., Cooper M. C., Tollerud E. J., 2014, *MNRAS*, 437, 1930
- Pohlen, M., & Trujillo, I. 2006, *A&A*, 454, 759
- Quilis V. & Trujillo I., 2012, *ApJ*, 752, L19
- Ragone-Figueroa, C., & Granato, G. L. 2011, *MNRAS*, 414, 3690
- Ricciardelli, E., Trujillo, I., Buitrago, F., & Conselice, C. J. 2010, *MNRAS*, 406, 230
- Ricciardelli E., Vazdekis A., Cenarro, A.J., Falcón-Barroso J., 2012, *MNRAS*, 424, 172
- Romanowsky, A. J., & Fall, S. M. 2012, *ApJS*, 203, 17
- Ruiz P., Trujillo I. & Mármol-Queraltó E., 2014, *MNRAS*, 442, 347
- Sales L., Lambas D. G., 2004, *MNRAS*, 348, 1236
- Sales L., Lambas D. G., 2005, *MNRAS*, 356, 1045
- Schlegel, D. J., Finkbeiner, D. P., & Davis, M. 1998, *ApJ*, 500, 525
- Steinmetz, M., & Muller, E. 1995, *MNRAS*, 276, 549
- Tal, T., Wake, D. A., van Dokkum, P. G., van den Bosch F. C., Schneider D. P., Brinkmann J., Weaver B. A., 2012, *Apj*, 746, 138
- Taylor, E. N., Franx, M., Glazebrook, K., Brinchmann J., van der Wel A., van Dokkum P. G., 2010, *ApJ*, 720, 723
- Trujillo I., Conselice C. J., Bundy K., Cooper M. C., Eisenhardt P., Ellis R. S., 2007, *MNRAS*, 382, 109
- Trujillo I., Cenarro A. J., de Lorenzo-Cáceres A., Vazdekis A., de la Rosa I. G., Cava A., 2009, *ApJ*, 692, L118
- Trujillo I., Ferreras I., de La Rosa I. G., 2011, *MNRAS*, 415, 3903
- Trujillo, I. Ferré-Mateu A., Balcells M., Vazdekis A., Sánchez-Blázquez P., 2014, *ApJ*, 780, L20
- van Dokkum, P. G., 2010, *ApJ*, 709, 1018
- Vazdekis A., Ricciardelli E., Cenarro A. J., Rivero-González J. G., Díaz-García L. A., Falcón-Barroso J., 2012, *MNRAS*, 424, 157
- Wang, W. T. 2013, *Acta Astron. Sinica*, 54, 584
- Wang, W., & White, S. D. M. 2012, *MNRAS*, 424, 2574
- Wild V., Walcher C. J., Johansson P. H., Tresse L., Charlot S., Pollo A., Le Fèvre O., de Ravel L., 2009, *MNRAS*, 395, 144
- Wuyts, S., Cox, T. J., Hayward, C. C., Franx M., Hernquist L., Hopkins P. F., Jonsson P., van Dokkum P. G., 2010, *ApJ*, 722, 1666
- Zavala, J., Okamoto, T., & Frenk, C. S. 2008, *MNRAS*, 387, 364